AD 746304

AFFDL-TR-70-138

# ROLLING RESISTANCE AND CARCASS LIFE OF TIRES OPERATING AT HIGH DEFLECTIONS

*FETERS SKELE*

TECHNICAL REPORT AFFDL-TR-70-138

D D C
AUG 9 1972
C

FEBRUARY 1972

Approved for public release; distribution unlimited.

Reproduced by
NATIONAL TECHNICAL
INFORMATION SERVICE
U S Department of Commerce
Springfield VA 22151

AIR FORCE FLIGHT DYNAMICS LABORATORY
AIR FORCE SYSTEMS COMMAND
WRIGHT-PATTERSON AIR FORCE BASE, OHIO 45433

45

NOTICE

When Government drawings, specifications, or other data are used for any purpose other than in connection with a definitely related Government procurement operation, the United States Government thereby incurs no responsibility nor any obligation whatsoever; and the fact that the government may have formulated, furnished, or in any way supplied the said drawings, specifications, or other data, is not to be regarded by implication or otherwise as in any manner licensing the holder or any other person or corporation, or conveying any rights or permission to manufacture, use, or sell any patented invention that may in any way be related thereto.

ACCESSION for
NTIS White Section ☑
DDC Buff Section ☐
UNANNOUNCED ☐
JUSTIFICATION .....
BY .....
DISTRIBUTION/AVAILABILITY CODES
Dist. AVAIL. and/or SPECIAL
A

Copies of this report should not be returned unless return is required by security considerations, contractual obligations, or notice on a specific document.

AIR FORCE: 27-3-72/150

UNCLASSIFIED
Security Classification

## DOCUMENT CONTROL DATA - R & D

*(Security classification of title, body of abstract and indexing annotation must be entered when the overall report is classified)*

| | |
|---|---|
| 1. ORIGINATING ACTIVITY (Corporate author)<br>Air Force Flight Dynamics Laboratory<br>Wright-Patterson Air Force Base, Ohio 45433 | 2a. REPORT SECURITY CLASSIFICATION<br>UNCLASSIFIED<br>2b. GROUP |

3. REPORT TITLE

ROLLING RESISTANCE AND CARCASS LIFE OF TIRES OPERATING AT HIGH DEFLECTIONS

4. DESCRIPTIVE NOTES (Type of report and inclusive dates)

5. AUTHOR(S) (First name, middle initial, last name)

Peter Skele

| | | |
|---|---|---|
| 6. REPORT DATE<br>February 1972 | 7a. TOTAL NO. OF PAGES<br>49 | 7b. NO. OF REFS |
| 8a. CONTRACT OR GRANT NO.<br>b. PROJECT NO. 5212<br>c.<br>d. | 9a. ORIGINATOR'S REPORT NUMBER(S)<br>AFFDL-TR-70-138<br>9b. OTHER REPORT NO(S) (Any other numbers that may be assigned this report) | |

10. DISTRIBUTION STATEM[redacted]

| | |
|---|---|
| 11. SUPPLEMENTARY NOTES | 12. SPONSORING MILITARY ACTIVITY<br>Air Force Flight Dynamics Laboratory<br>Wright-Patterson AFB, Ohio 45433 |

13. ABSTRACT


The purpose of this study was to determine the effects of tire deflection on rolling resistance resistance and tire life. The tests were conducted on a standard 84-inch diameter aircraft tire dynamometer. Some qualitative effects of deflection were determined.

The rolling resistance of a pneumatic tire subjected to a load acting through the wheel axis and normal to the contact patch plane is a function of velocity, deflection, and carcass temperature. When the load and carcass temperature are held constant, rolling resistance increases with increasing deflection and increasing velocity. For a constant deflection and carcass temperature, rolling resistance decreases with increasing inflation pressure. Experimental data from this study indicate that increasing carcass temperature while maintaining a constant deflection results in decreasing rolling resistance.

Tire life as characterized by carcass durability is highly dependent on deflection for 9.50-16 and 12.50-16 size tires. However, at high deflections, expandable (folding sidewall) tires of these sizes last significantly longer than do conventional construction bias ply tires. At rated deflections, i.e., deflections resulting from rated loads and inflation pressures, and for the larger size (17.00-20, 20.00-20) tires, no significant difference in tire life due to deflection or construction was evident within the range of test cycles undergone.


DD FORM 1 NOV 65 1473

UNCLASSIFIED
Security Classification

UNCLASSIFIED
Security Classification

| 14 KEY WORDS | LINK A ROLE | LINK A WT | LINK B ROLE | LINK B WT | LINK C ROLE | LINK C WT |
|---|---|---|---|---|---|---|
| Tires | | | | | | |
| Tire Wear | | | | | | |
| Friction | | | | | | |
| Rubber Friction | | | | | | |
| Rolling Resistance | | | | | | |
| Tire Flotation | | | | | | |

ib

☆U.S.Government Printing Office: 1972 — 759-084/ :51

UNCLASSIFIED
Security Classification

AFFDL-TR-70-138

# ROLLING RESISTANCE AND CARCASS LIFE OF TIRES OPERATING AT HIGH DEFLECTIONS

*PETERS SKELE*

[redacted]

ic

# FOREWORD

This report is the result of an in-house effort under ASD (ASNFL) Project No. 5212 "Improved Flotation for Tactical Aircraft." The work was carried out in the Landing Gear Group of the Mechanical Branch, Vehicle Equipment Division, Air Force Flight Dynamics Laboratory, Wright-Patterson Air Force Base, Ohio. This report was prepared by Mr. Peters Skele (FDFM).

This report was submitted by the author in April 1970.

This technical report has been reviewed and is approved.

K. H. Digges

KENNERLY H. DIGGES
Chief, Mechanical Branch
Vehicle Equipment Division
Air Force Flight Dynamics Laboratory

## ABSTRACT

The purpose of this study was to determine the effects of tire deflection on rolling resistance and tire life. The tests were conducted on a standard 84-inch diameter aircraft tire dynamometer. Some qualitative effects of deflection were determined.

The rolling resistance of a pneumatic tire subjected to a load acting through the wheel axis and normal to the contact patch plane is a function of velocity, deflection, and carcass temperature. When the load and carcass temperature are held constant, rolling resistance increases with increasing deflection and increasing velocity. For a constant deflection and carcass temperature, rolling resistance decreases with increasing inflation pressure. Experimental data from this study indicate that increasing carcass temperature while maintaining a constant deflection results in decreasing rolling resistance.

Tire life as characterized by carcass durability is highly dependent on deflection for 9.50-16 and 12.50-16 size tires. However, at high deflections, expandable (folding sidewall) tires of these sizes last significantly longer than do conventional construction bias ply tires. At rated deflections, i.e., deflections resulting from rated loads and inflation pressures, and for the larger size (17.00-20, 20.00-20) tires, no significant difference in tire life due to deflection or construction was evident within the range of test cycles undergone.

TABLE OF CONTENTS


| SECTION | | PAGE |
|---|---|---|
| I | INTRODUCTION | 1 |
| II | ROLLING RESISTANCE | 2 |
| | 1. A Method of Determining Rolling Resistance on the Dynamometer | 2 |
| | 2. Test Procedure | 5 |
| | 3. Results | 6 |
| III | TIRE LIFE (CARCASS DURABILITY) | 16 |
| | 1. Derivation of Test Conditions | 16 |
| | 2. Results | 20 |
| IV | CONCLUSIONS AND RECOMMENDATIONS | 27 |
| APPENDIX | MISSION CYCLE TEST CURVES | 29 |


Preceding page blank

# ILLUSTRATIONS


| FIGURE | | PAGE |
|---|---|---|
| 1. | Free Body Diagrams for Two Cases of Rolling Motion | 4 |
| 2. | Freewheeling Flywheel | 4 |
| 3. | Flywheel and Tire With Mutual Reaction Forces | 4 |
| 4. | Rolling Resistance vs Velocity: 9.50-16/10 PR (10,000 lb. Applied Load, 80°F Mean Temperature) | 8 |
| 5. | Rolling Resistance vs Velocity: 9.50-16/10 PR (30% Deflection, 80°F Mean Temperature) | 9 |
| 6. | Rolling Resistance vs Velocity: 9.50-16/10 PR (35% Deflection, 80°F Mean Temperature) | 10 |
| 7. | Rolling Resistance vs Velocity: 9.50-16/10 PR (10,000 lb. Applied Load, 30% Deflection) | 11 |
| 8. | Rolling Resistance vs Velocity: 17.00-20/22 PR (24,000 lb. Applied Load, 80°F Mean Temperature) | 12 |
| 9. | Rolling Resistance vs Velocity: 20.00-20/22 PR (33,000 lb. Applied Load, 80°F Mean Temperature) | 13 |
| 10. | Rolling Resistance vs Velocity: 17.00-20 Expandable (24,000 lb. Applied Load, 80°F Mean Temperature) | 14 |
| 11. | Rolling Resistance vs Velocity: 20.00-20 Expandable (33,000 lb. Applied Load, 80°F Mean Temperature) | 15 |
| 12. | Static Aircraft Loads | 16 |
| 13. | Main Gear Impact Loads | 18 |
| 14. | Nose Gear Loads During Landing Deceleration | 19 |
| 15. | Mission Takeoff: C-123 NLG Tire (9.50-16) | 30 |
| 16. | Mission Landing: C-123 NLG Tire (9.50-16) | 31 |
| 17. | Mission Takeoff: C-123 MLG Tire (17.00-20) | 32 |
| 18. | Mission Landing: C-123 MLG Tire (17.00-20) | 33 |
| 19. | Mission Takeoff: C-130 NLG Tire (12.50-16) | 34 |
| 20. | Mission Landing: C-130 NLG Tire (12.50-16) | 35 |

ILLUSTRATIONS (Contd)


| FIGURE | | PAGE |
|---|---|---|
| 21. | Mission Takeoff: C-130 MLG Tire (20.00-20) | 36 |
| 22. | Mission Landing: C-130 MLG Tire (20.00-20) | 37 |


TABLES


| TABLE | | |
|---|---|---|
| I | C-123 and C-130 Parameters | 20 |
| II | Mission Cycle Test Results | 21 |

## SYMBOLS

| | |
|---|---|
| $F$ | Reaction force between the dynamometer flywheel and the tire/wheel assembly acting tangential to the flywheel |
| $F_i$ | Instantaneous aircraft ground reaction |
| $F_L$ | Aerodynamic lift force at touchdown |
| $F_R$ | Rolling resistance force |
| $F_s$ | Static aircraft ground reaction |
| $I_1$ | Mass moment of inertia of the dynamometer flywheel |
| $I_2$ | Mass moment of inertia of the tire/wheel assembly |
| $L$ | Load applied at the tire/wheel assembly axle |
| $L_1$ | Distance of the nose gear from the center of gravity |
| $L_2$ | Distance of the main gear from the center of gravity |
| $L_i$ | Instantaneous aerodynamic lift force |
| $M$ | Aircraft mass |
| $M_1$ | A moment acting on the dynamometer flywheel due to bearing friction |
| $M_2$ | A moment acting on the tire/wheel assembly due to rolling resistance |
| $R_c$ | Rolling resistance coefficient |
| $R_m$ | Total reaction at the main gear position |
| $R_{mi}$ | Main gear impact load |
| $R_n$ | Total reaction at the nose gear position |
| $V_i$ | Instantaneous ground velocity |
| $V_t$ | Takeoff velocity |
| $W$ | Aircraft gross weight |
| $a$ | Braking deceleration |
| $d$ | Shock strut stroke plus tire deflection |
| $e$ | Displacement of normal component of ground reaction |
| $g$ | Acceleration due to gravity |

Center of gravity

| | |
|---|---|
| $h$ | Distance of the aircraft center of gravity from the ground |
| $k$ | Constant of proportionality |
| $l$ | Shock strut stroke |
| $r_1$ | Radius of dynamometer flywheel |
| $r_2$ | Effective rolling radius of the tire/wheel assembly |
| $t$ | Time |
| $v$ | Aircraft sink speed at touchdown |
| $\alpha_1$ | Flywheel angular displacement, no tire loads present |
| $\alpha_2$ | Flywheel angular displacement, tire loads present |
| $\theta$ | Angular displacement of the tire/wheel assembly |
| $x_1$ | Vertical position coordinate at touchdown |
| $x_2$ | Vertical position coordinate at maximum strut deflection |

# SECTION I

# INTRODUCTION

Current Air Force missions require that aircraft operate from unprepared or semi-prepared airstrips. In many cases, aircraft operating from such strips (particularly cargo aircraft) experience severe flotation problems.

Previous work by the Air Force Flight Dynamics Laboratory and others had shown that flotation could be substantially improved by lowering tire inflation pressure, resulting in a lower mean contact pressure. However, the effects of the resulting high deflections on such properties as tire life and rolling resistance were known only in a general qualitative fashion.

The purpose of this effort was to determine more specifically the dependency of tire life (carcass durability) and rolling resistance on tire deflection.

The tires selected for this study were the 9.50-16 (C-123 nose), 17.00-20 (C-123 main), 12.50-16 (C-130 nose), and 20.00-20 (C-130 main) sizes. Both conventional construction and folding sidewall tires were tested.

# SECTION II

# ROLLING RESISTANCE

## 1. A METHOD OF DETERMINING ROLLING RESISTANCE ON THE DYNAMOMETER

Any rolling object, whether in steady state or under acceleration, experiences a certain resistance tending to retard its motion. This phenomenon is explained in elementary mechanics in the following way.

Consider the steady state rolling of a solid elastic cylinder on a flat surface (Figure 1a). From observation, we know that a force F is required to keep it in motion. Therefore, there must be a resisting force acting through the center of gravity opposing the motion. This is the force N acting at a small angle B. The angle B is a result of deformations of the two bodies. Equating horizontal forces and making the small angle assumption, we arrive at

$$F = \frac{Ls}{r}$$

We call F the rolling resistance force.

Now, consider a tire in general rolling motion. A free body schematic is shown in Figure 1b. Here the total resisting force is represented by its two orthogonal components. The vertical component is displaced from the tire centerline by an amount e, which is on an order of several inches for pneumatic tires. Summing moments and intertial terms, we arrive at

$$Fr_2 - Le + I_2\ddot{\theta} = 0 \qquad (1)$$

Next, let us look at a dynamometer flywheel decelerating due to friction forces. A free body diagram is depicted in Figure 2. Again summing moments and inertial terms, we arrive at

$$-M_1 + I_1\ddot{\alpha}_1 = 0 \qquad (2)$$

Finally, consider the ease of a tire loaded against a rotating flywheel, both decelerating due to friction effects and tire rolling resistance. The free body

diagrams for this case are shown in Figure 3. From Figure 3a, summing moments and inertial terms results in

$$-M_1 - Fr_1 - Le + I_1 \ddot{\alpha}_2 = 0 \tag{3}$$

Making a similar summation from Figure 3b, we get

$$Fr_2 - Le + I_2 \ddot{\theta} = 0 \tag{4}$$

In Equation 4 we have assumed that the bearing friction is small as compared to the other forces present.

We now want to arrive at an equation for F containing only variables pertaining to the dynamometer flywheel. We do this because the dynamometer wheel is more readily instrumented.

Substracting Equation 4 from Equation 3 and rearranging terms results in

$$-F(r_1 + r_2) = M_1 - I_1 \ddot{\alpha}_2 + I_2 \ddot{\theta} \tag{5}$$

Making the substitution $M = I_1 \ddot{\alpha}_1$ from Equation 2, we get

$$-F(r_1 + r_2) = I_1 \ddot{\alpha}_1 - I_1 \ddot{\alpha}_2 + I_2 \ddot{\theta} \tag{6}$$

We still have the tire variable $\ddot{\theta}$ to eliminate. We do this by making the approximation

$$\ddot{\theta} = \frac{r_1}{r_2} \ddot{\alpha}_2 \tag{7}$$

Making this substitution, Equation 6 becomes

$$-F(r_1 + r_2) = I_1 \ddot{\alpha}_1 - I_1 \ddot{\alpha}_2 + I_2 \frac{r_1}{r_2} \ddot{\alpha}_2 \tag{8}$$

Collecting terms, we get

$$-F(r_1 + r_2) = -(I_1 - I_2 \frac{r_1}{r_2}) \ddot{\alpha}_2 + I_1 \ddot{\alpha}_1 \tag{9}$$

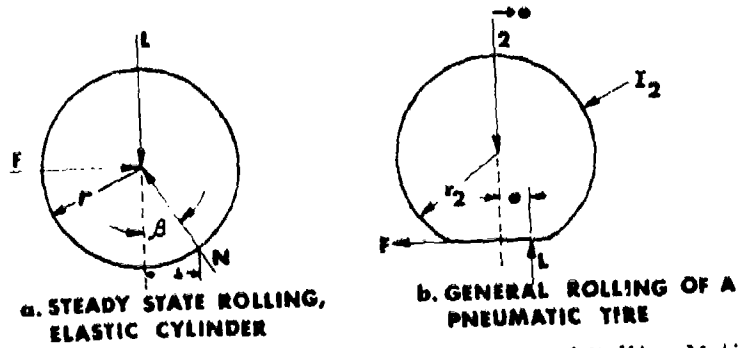


Figure 1. Free Body Diagrams for Two Cases of Rolling Motion

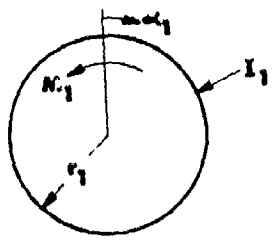


Figure 2. Freewheeling Flywheel

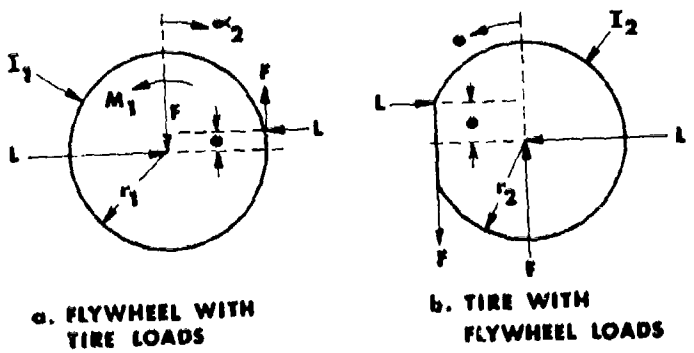


Figure 3. Flywheel and Tire With Mutual Reaction Forces

or

$$-F(r_1 + r_2) = -I_1\left(1 - \frac{I_2}{I_1}\frac{r_1}{r_2}\right)\ddot{\alpha}_2 + I_1\ddot{\alpha}_1 \tag{10}$$

A further simplification of Equation 10 is possible since

$$\left[\left(\frac{I_2}{I_1}\right)\left(\frac{r_1}{r_2}\right)\right]_{max} \simeq 6 \cdot 10^{-3} << 1 \tag{11}$$

thus

$$-F(r_1 + r_2) = -I_1\ddot{\alpha}_2 + I_1\ddot{\alpha}_1 \tag{12}$$

Collecting terms and dividing both sides by $-(r_1 + r_2)$, we get

$$F = I_1(\ddot{\alpha}_2 - \alpha_1)/(r_1 + r_2) \tag{13}$$

This then is the rolling resistance force in terms of the easily measured quantities $I_1, r_1, r_2, \ddot{\alpha}_2$, and $\ddot{\alpha}_1$.

We can define a dimension less rolling resistance coefficient by dividing Equation 13 by the applied tire load. Mathematically, we can say

$$R_c = \frac{F}{L} = \frac{I_1(\ddot{\alpha}_2 - \ddot{\alpha}_1)}{L(r_1 + r_2)} \tag{14}$$

## 2. TEST PROCEDURE

Test procedure for each tire was as follows: prior to testing, the tire was put through the standard stretch and break in procedure outlined in MIL-T-5041E. The tire/wheel assembly was then mounted on the dynamometer load carriage and the inflation pressure was adjusted to get the desired deflection at a load within the static load range of that tire on the aircraft. In order to minimize the effects of heat and pressure buildup in the tire during the test, tire time on the dynamometer was kept at a minimum. This was accomplished in the following way: The ground velocity range of each aircraft was divided into

three parts, establishing starting speeds. The flywheel was then brought up to the desired starting speed and the drive motor was shut off. The tire was loaded against the flywheel and flywheel velocity as a function of time was recorded. Tire time on the flywheel was on the order of 30 seconds. Typical temperature (contained air) rise was 5°F and typical pressure increase was 2 PSI.

The raw data was gathered in the following way: a magnetic proximity sensor detected the passing of regularly space gear teeth on the flywheel shaft. The resulting signal was used to open and close a gate in an Events Per Unit Time (EPUT) Meter, allowing the number of cycles of a signal from an internal crystal to be counted. Since the diameter of the flywheel is known, this data is directly convertible to velocity. The sampling rate was provided by a preset controller, which reset the EPUT meter every two or five seconds, depending on flywheel velocity. The control signal used by the preset controller was a 60 Hz line voltage from the facility electrical system.

The raw data was converted to angular velocity versus time and then smoothed, using an averaging technique. The result was then used to perform the calculations in Equations 13 and 14. The final printout was a tabulation of $R_c$ versus velocity with units of miles per hour.

## 3. RESULTS

Figures 4 through 11 are the results of the rolling resistance tests in graphical form. The data points in these plots exhibit considerable scatter. This scatter is caused primarily by the presence of two phenomena during the test runs: electromagnetic noise introduced by the large electrical dynamometer drive motors and poor tire load stability. The high level of electromagnetic noise in the test area caused spurious signals to be recorded by the instrumentation, often obscuring trends in the desired signal. The observed variation in tire loads has two possible sources: 1) the tire/wheel assembly unbalance due to contained air lines could cause the noticeable cyclic load variation, and 2) the vibration from the wheel unbalance could allow the load piston to overcome friction forces acting between the piston and cylinder wall, causing the piston to relocate itself in a neutral position. Since rolling resistance is highly

dependent on tire deflection, even a slight change in piston position during the test run is significant.

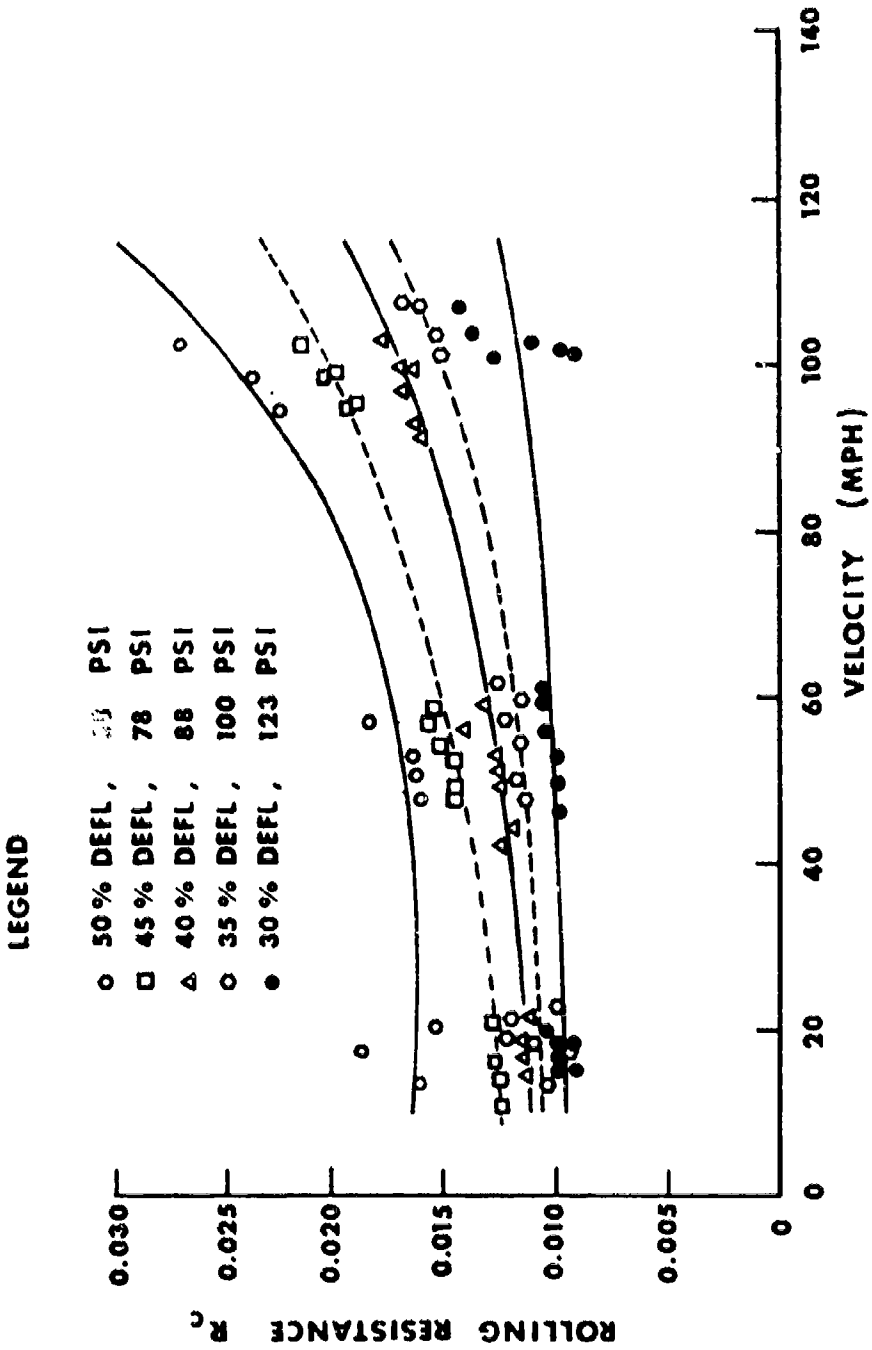


Figure 4. Rolling Resistance vs Velocity: 9.50-16/10 PR (10,000 lb. Applied Load, 80°F Mean Temperature)

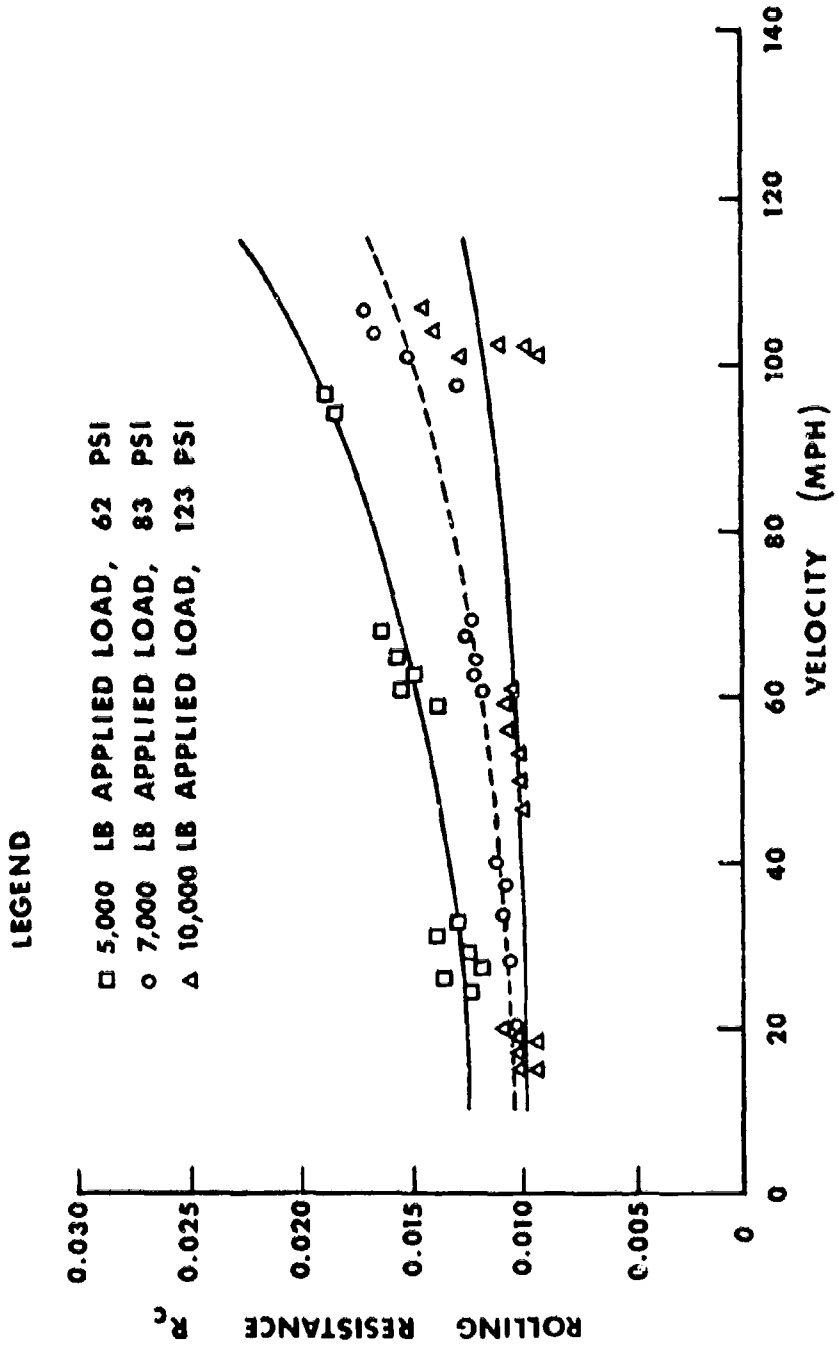


Figure 5. Rolling Resistance vs Velocity: 9.50-16/10 PR (30% Deflection, 80°F Mean Temperature)

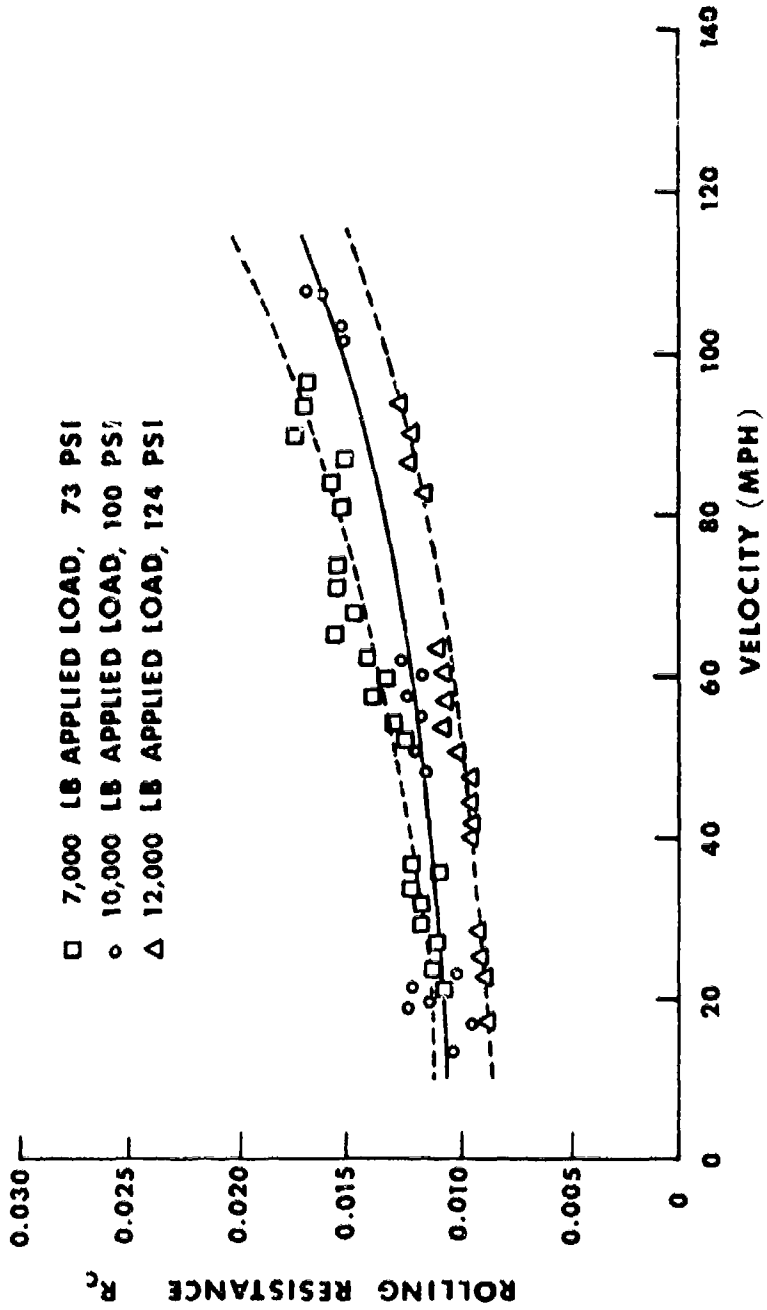


Figure 6. Rolling Resistance vs Velocity: 9.50-16/10 PR (35% Deflection, 80°F Mean Temperature)

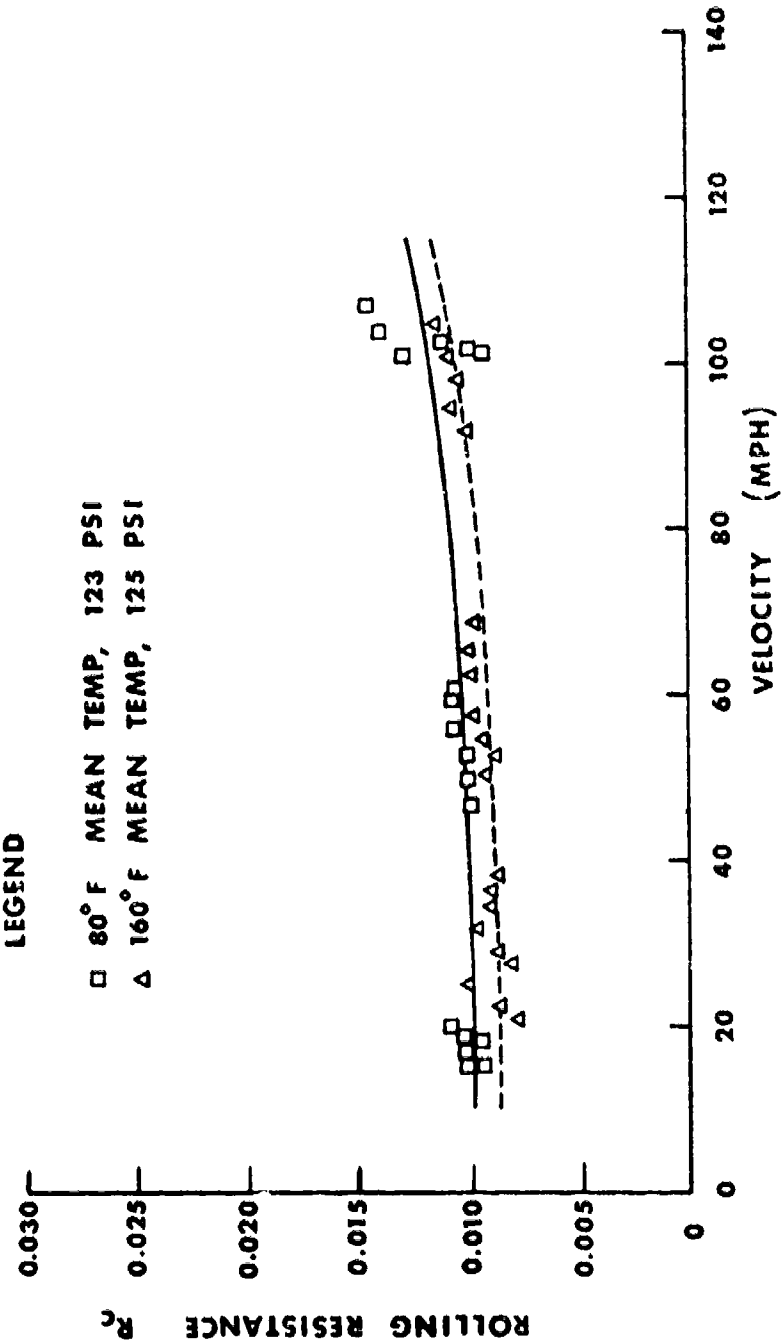


Figure 7. Rolling Resistance vs Velocity: 9.50-16/10 PR (10,000 lb. Applied Load, 30% Deflection)

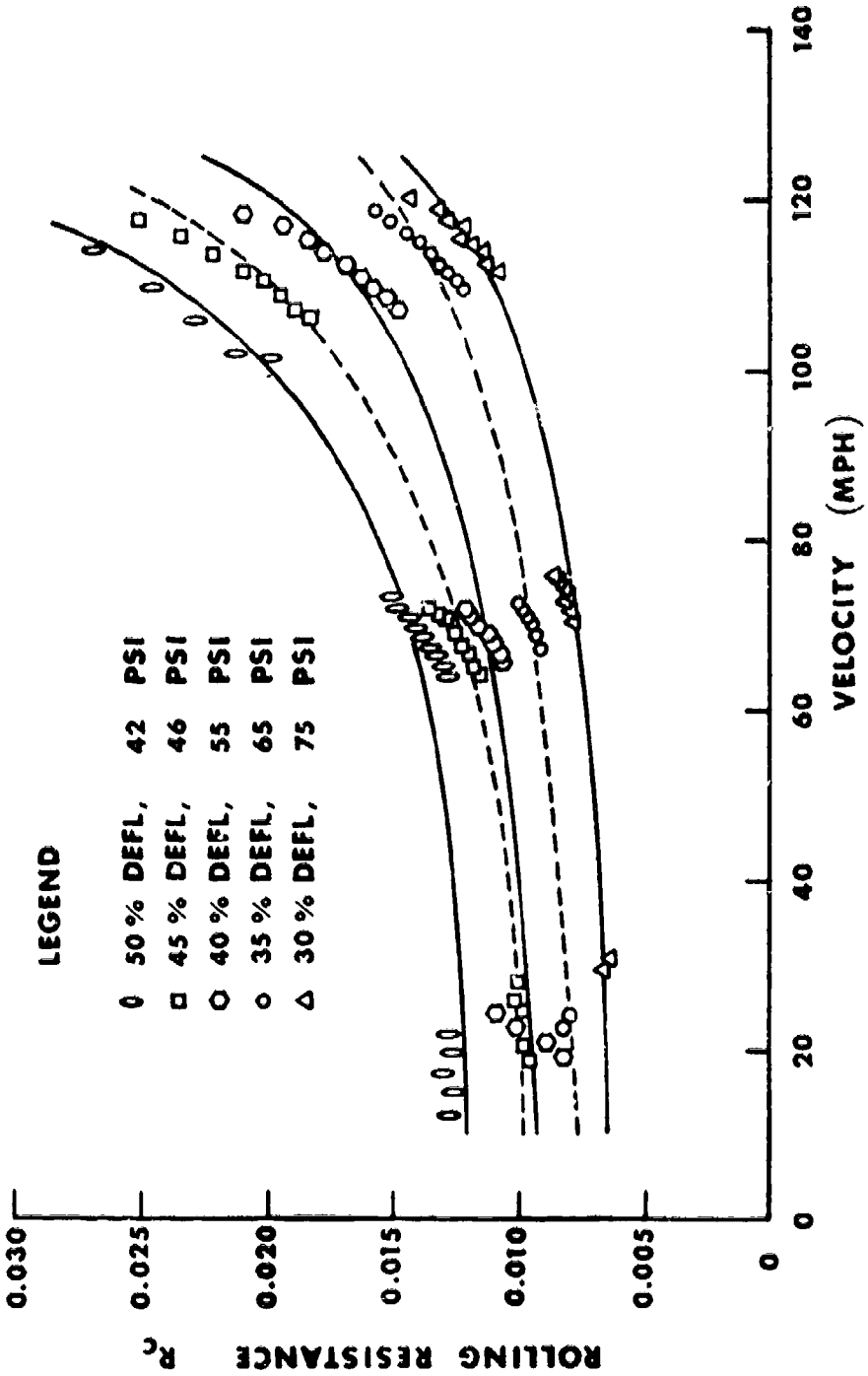


Figure 8. Rolling Resistance vs Velocity: 17.00-20/22 PR (24,000 lb. Applied Load, 80°F Mean Temperature)

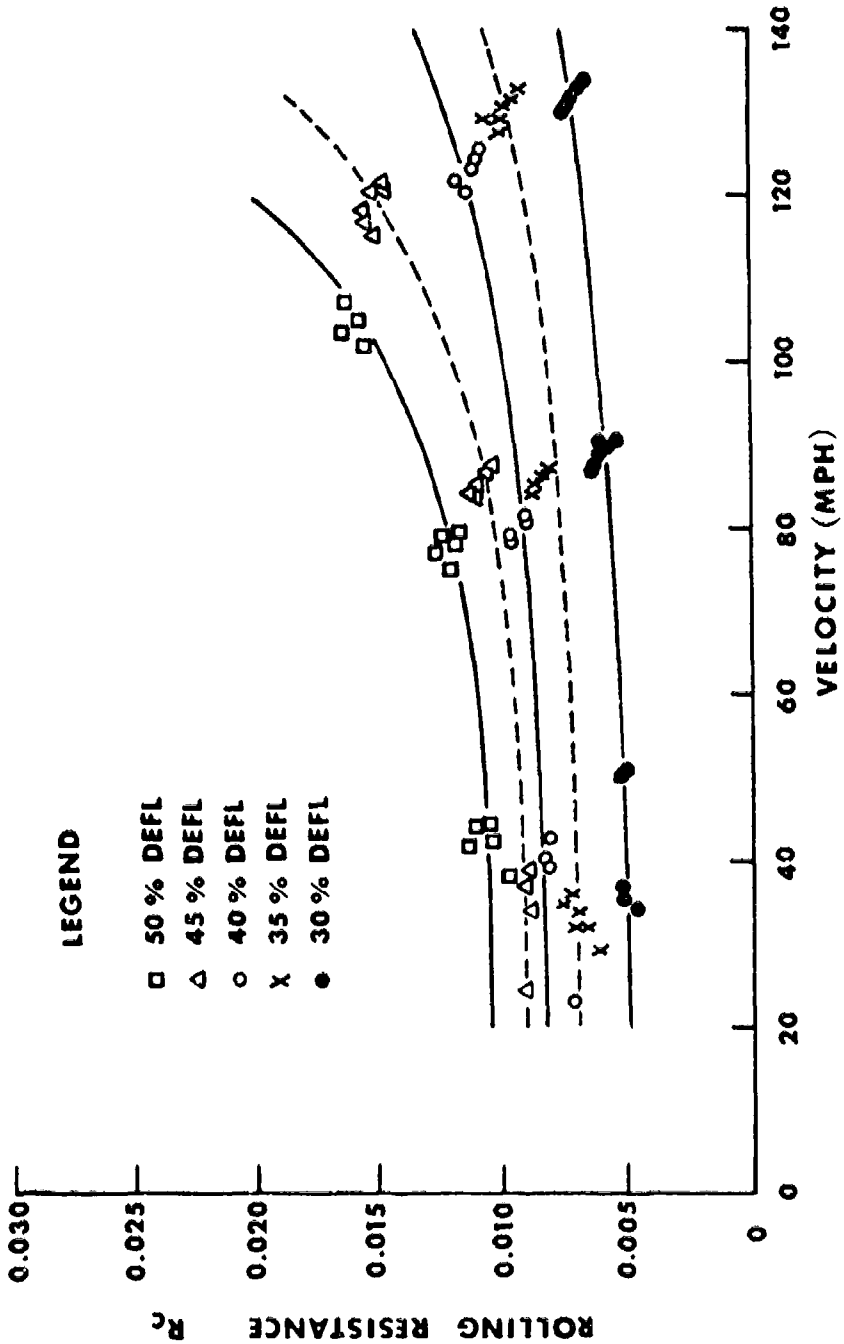


Figure 9. Rolling Resistance vs Velocity: 20.00-20/22 PR (33,000 lb. Applied Load, 80°F Mean Temperature)

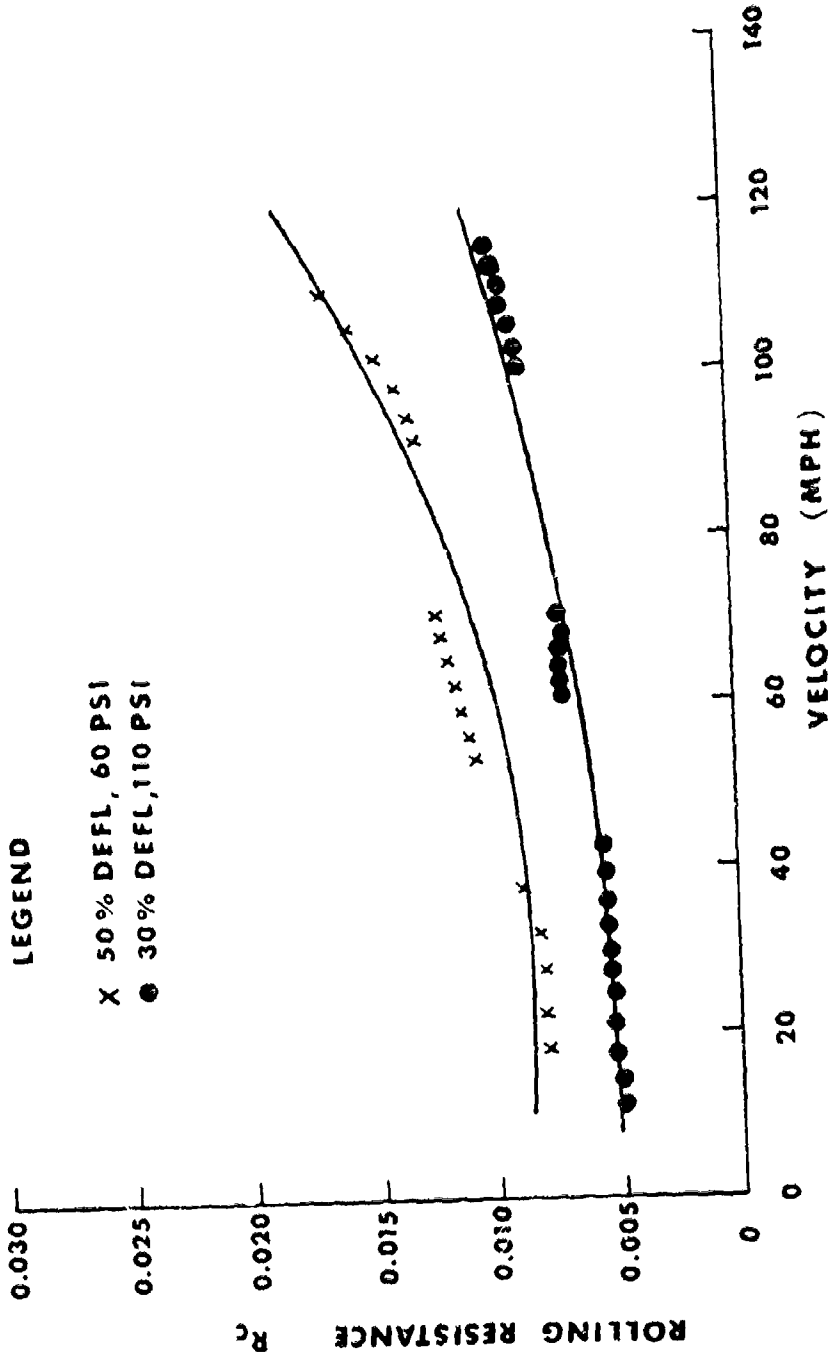


Figure 10. Rolling Resistance vs Velocity: 17.00-20 Expandable (24,000 lb. Applied Load, 80°F Mean Temperature)

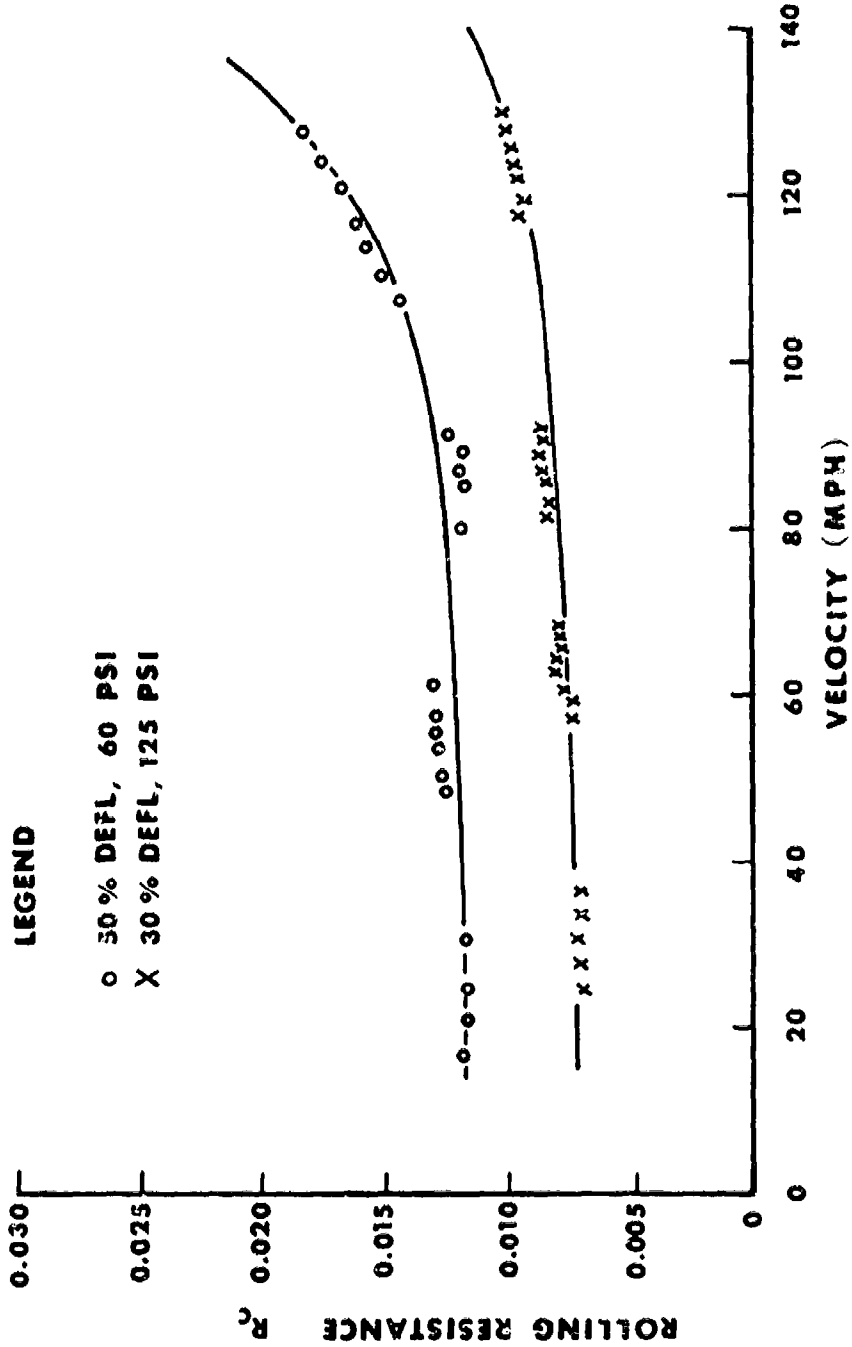


Figure 11. Rolling Resistance vs Velocity: 20.00-20 Expandable (33,000 lb. Applied Load, 80°F Mean Temperature)

# SECTION III

# TIRE LIFE (CARCASS DURABILITY)

## 1. DERIVATION OF TEST CONDITIONS

In this portion of the test program, the various tires were subjected to simulated assault missions; i.e. the loads and speeds that a particular tire undergoes during typical takeoffs and landings were reproduced on the dynamometer to the extent possible with the stated assumptions below.

Tire loads for the taxi-takeoff condition were calculated in the following manner (Reference Figure 12):

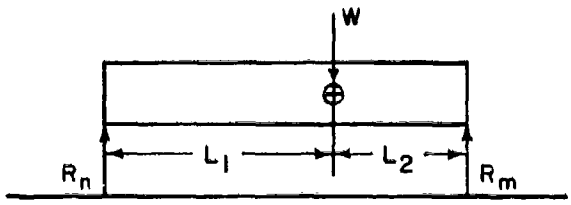


Figure 12. Static Aircraft Loads

Treating the aircraft as a simply supported beam, equilibrium of vertical forces yields

$$R_n + R_m = W \tag{15}$$

and equilibrium of moments about the main landing gear (MLG) yields

$$(L_1 + L_2) R_n = WL_2 \tag{16}$$

Solving Equations 15 and 16 for $R_n$ and $R_m$ results in

$$R_n = W \left( \frac{L_2}{L_1 + L_2} \right) \tag{17}$$

and

$$R_m = W \left( \frac{L_1}{L_1 + L_2} \right) \tag{18}$$

where $R_n$ is the total reaction at the nose gear (NG) position and $R_m$ is the total reaction at the main gear position. Equations 17 and 18 give the static reactions. These values can also be used for the taxi portion of the taxi-takeoff condition since aerodynamic forces are negligible at taxi speeds.

If we assume that the center of lift and the center of gravity are coincident, that the aerodynamic control surfaces are fixed, and that the aircraft attitude remains constant, tire loads during takeoff can be calculated in the following way:

From elementary aerodynamics, under the above conditions, we can say that the instantaneous lift is proportional to the square of the velocity; i.e.,

$$L_i = kV_i^2 \tag{19}$$

Instantaneous total aircraft ground reaction is then the difference between the static reaction and instantaneous lift;

$$F_i = F_s - kV_i^2 \tag{20}$$

But at the moment of lift off, ground reaction is zero. Thus,

$$F_s = kV_t^2 \tag{21}$$

where $V_t$ is the takeoff velocity. Solving for k in Equation 21, substituting the result into Equation 20 and factoring yields

$$F_i = F_s \left(1 - \frac{V_i^2}{V_t^2}\right) \tag{22}$$

Equation 22 can be used to calculate individual tire loads by replacing $F_s$ with the appropriate static tire loads since we assumed that the aircraft attitude was constant. The values of $V_i$ and $V_t$ in Equation 22 were obtained from performance data in the aircraft T. O.'s and from flight test data.

Tire loads for the land-taxi condition were determined as follows: For the purpose of this calculation, it was assumed that the kinetic energy of the aircraft due to the vertical component of its velocity was entirely absorbed by the main

gear shock absorbers, and that the shock absorber efficiency was 100%, i.e., the load-stroke curve was a step function. Figure 13 is a representation of the aircraft with the above assumptions.

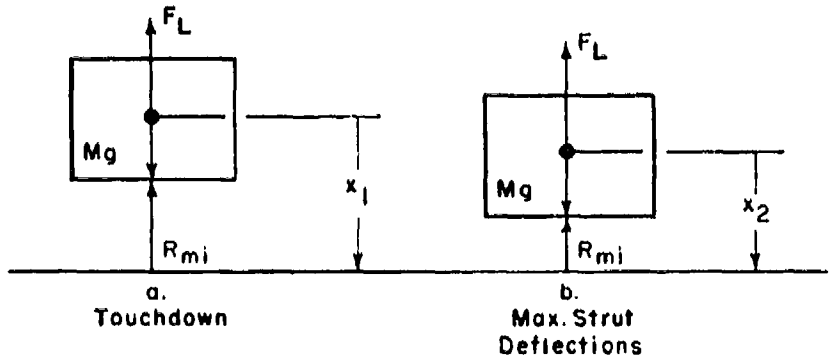


Figure 13. Main Gear Impact Loads

Equating the change in kinetic and potential energy to the work done by the external forces between states a) and b) results in

$$\frac{1}{2} M(\dot{x}_2^2 - \dot{x}_1^2) + Mg(x_2 - x_1) = (F_L + R_{mi})(x_2 - x_1) \tag{23}$$

Rewriting Equation 23 using the substitutions $v^2 = \dot{x}_1^2 - \dot{x}_2^2$, $\ell = x_1 - x_2$ results in

$$\frac{1}{2} Mv^2 + Mg\ell = (F_L + R_{mi})\ell \tag{24}$$

where v is the sink speed at touchdown, $\ell$ is the shock strut stroke, $F_2$ is the lift force at touchdown, and $R_{mi}$ is the main gear impact load. For the ideal assault landing aircraft stall speed is reached at the moment of touchdown. Therefore, $F_L$ in Equation 24 is zero. Rewriting Equation 24 and solving for $R_{mi}$ yields

$$R_{mi} = \frac{\frac{1}{2} Mv^2 + Mg\ell}{\ell} \tag{25}$$

Equation 25 establishes an upper bound for the main landing gear impact loads. To establish a lower bound, rewrite Equation 24 to get

$$\frac{1}{2} Mv^2 + Mgd = (F_L + R_{mi})d \tag{26}$$

where d is the shock strut stroke plus tire deflection. Solving Equation 26 for $R_{mi}$ yields

$$R_{mi} = \frac{\frac{1}{2} M_v^2 + Mgd}{d} - F_L \tag{27}$$

Taxi loads for the main gear can be calculated using Equation 18 where W is now the landing gross weight, and the effects of braking forces are ignored.

Nose gear loads during landing deceleration can be calculated as follows:

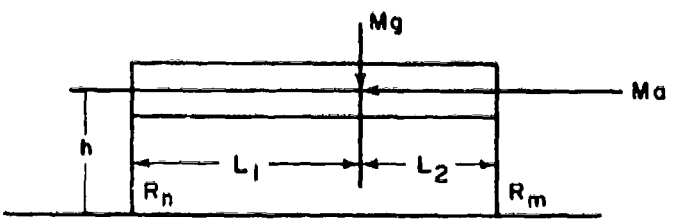


Figure 14. Nose Gear Loads During Landing Deceleration

Referring to Figure 14, summation of moments about $R_m$ results in

$$- Mah - MgL_2 + R_n (L_1 + L_2) = 0 \tag{28}$$

Solving for $R_n$ yields

$$R_n = \frac{Mah + MgL_2}{L_1 + L_2} \tag{29}$$

where a is the deceleration o during landing Equation 29 ignores the effects of pitching moment of inertia of the aircraft, lift forces, and assumes that no reverse thrust is used, thus giving conservative values for the nose gear loads.

The following values were used to calculate the load profiles.

TABLE I

C-123 AND C-130 PARAMETERS

| | | C-123 | C-130 |
|---|---|---|---|
| Taxi Takeoff Condition | W | 60,000 lbs. | 155,000 lbs. |
| | $L_1$ | 222 in* | 247 in* |
| | $L_2$ | 56 in* | 41 in* |
| | h | 105 in | 165 in |
| | $V_t$ | 120 mph | 132 mph |
| | Takeoff Distance | 2500 ft. | 2500 ft. |
| Land Taxi Condition | W | 53,000 lbs. | 140,000 lbs. |
| | $\sim$ | 10 ft/sec | 10 ft/sec |
| | a | 9.1 ft/sec$^2$ | 7 ft/sec$^2$ |
| | d | 20.3 inch | 22 inch |
| | $F_L$ | 53,000 lbs. | 140,000 lbs. |
| | Landing Distance | 2,000 ft. | 2,500 ft. |

* Maximum aircraft center of gravity. Values used for the C-130 measured from midpoint of main gear struts.

The velocity time histories were obtained from the aircraft T. O.'s and flight test data. The load and speed time histories used for the mission cycle tests are seen in Figures 15 through 22 in the Appendix.

## 2. RESULTS

The purpose of this part of the test program was to determine the effects of high deflections on tire life, i.e., carcass durability. To this end, the tires were subjected to simulated assault missions as derived in the previous section. The tires were tested at deflections varying from 30% to 50%. The load at which the deflections were established was the taxi load of the particular condition the tire was undergoing, i.e. takeoff or landing condition. The results are tabulated by size and type in Table II.

TABLE II

MISSION CYCLE TEST RESULTS

| TIRE SIZE AND TYPE | TIRE NO. | PERCENT DEFL. | MEAN INFL. PRESSURE | T.T.O.* COMPLETED | L.T.** COMPLETED |
|---|---|---|---|---|---|
| 9.50-16/10PR Conventional Construction | 1 | 50 | 37 | 79 | 10 |
| | 2 | 45 | 45 | 10 | 1 |
| | 3 | 45 | 44 | 30 | 30 |
| | 4 | 40 | 53 | 260 | 251 |
| | 5 | 30 | 74 | 500 | 500 |
| 9.50-16 Expandable | 1 | 50 | 45 | 114 | 110 |
| | 2 | 50 | -- | -- | -- |
| 17.00-20/22PR Conventional Construction | 1 | 45 | 74 | 334 | 330 |
| | 2 | 45 | 76 | 498 | 490 |
| | 3 | 35 | 98 | 300 | 300 |
| 17.00-20 Expandable | 1 | 50 | 75 | 150 | 150 |
| | 2 | 50 | 72 | 150 | 150 |
| 12.50-16/12PR Conventional Construction | 1 | 43 | 38 | 10 | 5 |
| | 2 | 35 | 46 | 90 | 86 |
| | 3 | 30 | 55 | 310 | 304 |
| 12.50-16 Expandable | 1 | 50 | 50 | 117 | 110 |
| | 2 | 50 | 50 | 150 | 150 |
| 20.00-20/22PR Conv. Constr. | 1 | 50 | 69 | 300 | 300 |
| | 2 | 35 | 95 | 300 | 300 |
| 20.00-20 Expandable | 1 | 50 | 73 | 150 | 150 |
| | 2 | 50 | 74 | 150 | 150 |

*Taxi-Takeoff **Land-Taxi

9.50-16/10 PR Conventional Construction

Tire 1 completed 79 taxi-takeoff cycles and 10 land-taxi cycles at 50% deflection before failure. Inspection revealed inner liner and cord rupture in the shoulder area. No damage was visible on the exterior surface of the tire. Typical contained air temperature rise during taxi-takeoff cycles was 19°F and during land-taxi cycles, typical rise was 48°F.

Tire 2 failed after 10 taxi-takeoff cycles and 1 land-taxi cycle at 45% deflection. Approximately 15% of the outboard sidewall and 50% of the inboard sidewall ruptured near the juncture of the sidewall and tread. Typical contained air temperature rise during taxi-takeoff cycles was 25°F. The temperature increased 64°F during the land-taxi cycles.

Tire 3 completed 30 mission cycles (30 each, TTO and LT) at 45% deflection before failure. Inspection revealed inner liner and cord rupture in the shoulder area. No exterior damage was visible. Typical contained air temperature rise during taxi-takeoff cycles was 23°F and during land-taxi cycles, typical rise was 79°F.

Tire 4 completed 260 taxi-takeoff cycles and 251 land-taxi cycles at 40% deflection before failure. Failure was due to rupture of the inner tube, apparently due to pinching at the high deflections encountered. Inspection of the tire revealed a large blister on the inboard sidewall of the tire and the testing was stopped. Typical contained air temperature rise during taxi-takeoff cycles was 18°F and during land-taxi cycles, typical rise was 50°F.

Tire 5 completed 500 mission cycles without failure. Contained air temperature was not measured due to loss of the commutator during the previous tire test. Sidewall temperature measured with a hand held probe immediately after completion of each run, showed a 10°F temperature rise during taxi takeoff cycles and a 20°F rise during land-taxi cycles on the average.

9.50-16 Expandable

Tire 1 completed 114 taxi-takeoff cycles and 110 land-taxi cycles. Testing was stopped due to large bulges on both sidewalls indicating ply separation. The sidewall bulges developed after 110 mission cycles. Tire deflection was 50%. Temperature data was not taken due to malfunction of the pyrometer. Folding quality was excellent for the first 50 mission cycles. Thereafter, folding time progressed from 10 sec. to 175 sec. Typical offset after 50 mission cycles was 1/2 inch. The term offset as used in this report is the displacement of the tread center plane from the wheel center plane.

Tire 2 failed by gross carcass rupture on the second rolling resistance run (at approximately 70 mph, 10,000 lb. load).

17.00-20/22 PR Conventional Construction

Tire 1 completed 334 taxi-takeoff cycles and 330 land-taxi cycles at 45% deflection without failure. Typical contained air temperature rise during

taxi-takeoff cycles was 18°F and during land-taxi cycles, the typical rise was 26°F. The peak load on the land-taxi cycles was 30,000 lbs. for this tire. The land-taxi peak load was changed to 40,000 lbs. for the remaining 17.00-20 tires.

Tire 2 completed 498 taxi-takeoff cycles and 490 land-taxi cycles at 45% deflection without failure. Contained air temperature rise during taxi-takeoff cycles was typically 19°F and during land-taxi cycles typical rise was 32°F.

Tire 3 completed 300 mission cycles at 35% deflection without failure. The contained air temperature increased 9°F typically during taxi-takeoff cycles and 15°F during land-taxi cycles.

17.00-20 Expandable

Tire 1 completed 150 mission cycles without failure. Deflection was 50%. Typical sidewall temperature rise during taxi-takeoff cycles was 17°F and typical rise during land-taxi cycles was 33°F. The tire folded 3 in. offset to the inboard side at start of testing and progressed to a 6 in. offset to the inboard at the end of testing. Cracks in the surface rubber in the fold area developed after 14 mission cycles. Ply separation was noticed after 100 taxi-takeoff cycles and 90 land taxi cycles in the form of two large bulges extending from the fold to the shoulder approximately 10 in. apart in the outboard sidewall. An attempted land-taxi after completion of the 150 mission cycles with the tire completely folded resulted in loss of bead seat and rupture of the sidewalls several places around the circumference of the tire.

Tire 2 completed 150 mission cycles without failure. Deflection was 50%. Sidewall temperature rise during taxi-takeoff cycles was 15°F typically. During land-taxi cycles the temperature rose 30°F typically. Folding quality was fair: offset progressed from 1/3 in. outboard at start of testing to 2 in. outboard at end of testing. Average fold time was on the order of 100 sec. Two small cracks developed in the tread area after 20 taxi-takeoff cycles and 10 land-taxi cycles. The crack dimensions after 150 mission cycles were .03 in. wide by 0.5 in. long by .12 in deep and .03 in. wide by 0.25 in. long by .12 in. deep.

12.50-16/12 PR Conventional Construction

Tire 1 completed 10 taxi-takeoff cycles and 5 land-taxi cycles at 43% deflection before failure. Failure was by sidewall rupture near the tire shoulder. Sidewall temperature rise during-taxi takeoff cycles was typically 17°F and during land-taxi cycles, temperature rise progressed from 20°F on the first run to 80°F on the last run.

Tire 2 completed 90 taxi-takeoff cycles and 80 land-taxi cycles at 35% deflection before failure. Inspection revealed inner liner and cord rupture in the shoulder area. No damage was visible on the exterior surface of the tire. Typical sidewall temperature rise during taxi-takeoff cycles was 9°F and during land-taxi cycles, typical rise was 40°F.

Tire 3 completed 310 taxi-takeoff cycles and 304 land-taxi cycles at 30% deflection before failure. Inspection revealed inner liner and cord rupture in the shoulder area. No exterior damage was visible. Typical sidewall temperature rise during taxi-takeoff cycles was 6°F and typical rise during land-taxi cycles was 33°F.

12.50-16 Expandable

Tire 1 completed 117 taxi-takeoff cycles and 110 land-taxi cycles at 50% deflection before failure. Failure occurred by carcass rupture in the inboard fold area several places around the tire circumference. Sidewall temperature rise during taxi-takeoff cycles was 33°F typically and during land-taxi cycles typical rise was 43°F. Folding quality was poor: folding time progressed from 120 sec. at test start to 25 min. for complete settling at end of testing. Offset progressed from zero to 1 in. in the same period. Some cracking of the surface rubber in the fold area developed after 96 mission cycles.

Tire 2 completed 150 mission cycles at a deflection of 50% without failure. Folding quality was excellent for the first 100 mission cycles. After the 100th mission cycle folding quality deteriorated until after 120 mission cycles, the tire folded completely offset to the inboard side. Temperature data is not available for this tire.

20.00-20/22 PR Conventional Construction

Tire 1 completed 300 mission cycles at 50% deflection without failure. Contained air temperature rise during both taxi-takeoff cycles and land-taxi cycles was typically 13°F.

Tire 2 completed 300 mission cycles at 35% deflection without failure. Contained air temperature rise during mission cycles was on the order of 10°F.

20.00-20 Expandable

Tire 1 completed 150 mission cycles at a deflection of 50% without failure. Typical sidewall temperature rise during taxi-takeoff cycles was 17°F and during land-taxi cycles the average rise was 21°F. Folding quality was extremely poor; i.e., the tire folded completely offset to either side.

Tire 2 completed 150 mission cycles without failure. Deflection was 50%. Sidewall temperature rise during taxi-takeoff cycles was 13°F on the average and during land-taxi cycles the average rise was 20°F. The tire folded completely offset to either side.

The 9.50-16 land-taxi load profile (Figure 16) shows a peak load of 10,350 lbs. This is erroneous. The load should rise to 9,150 lbs. and stay constant at that level for the duration of the deceleration. The first four 9.50-16/10 PR tires had completed the test program before this error was discovered. It was decided to continue to use this profile in order not to lose the accumulated data, since the purpose of these tests was to gain knowledge of relative performance; i.e. 50% deflection vs 30%, 45% deflection vs 30% etc.

The peak loads on the main landing gear land-taxi curves were arbitrarily chosen at 40,000 lbs., the maximum load capability of the 84 inch dynamometer. This value lies between the upper and lower bound values calculated in Equations 25 and 27. The rise times of all the loads are determined by the maximum load application rate of the dynamometer load carriage.

It should be noted that the mission cycle tests as performed on the dynamometer are indicative primarily of the ability of the carcass to withstand the high deflections encountered. Actual tire life in the field is expected to be considerably shorter due to a much higher wear rate and tread cutting. Also, it is important to note that loads due to braking and camber on the main gear tires, and camber and yaw loads on the nose gear tires were not accounted for. These loads become increasingly important as tire deflection increases. In drawing any conclusions concerning field use at lower than rated inflation pressures, a factor to consider is that several of the nose gear tires tested failed by rupture of the inner liner and several of the inner plys, with no visible exterior damage. Failure was usually noted by an abrupt pressure loss, indicating inner tube failure due to abrasion or pinching by the ruptured plies. Thus, in order to operate tires at high deflections on aircraft, some form of nondestructive testing would be required, both before initial use and between every mission.

Table II shows that for the nose gear tires (9.50-16 and 12.50-16), tire life as determined by carcass durability is sharply dependent on deflection, and that for a given deflection, the expandable tires have a greater life expectancy. Observation of the tires under load show that the conventional construction tires tend to buckle in the sidewall at high deflection (>40%), while the expandable tires do not. At deflections where sidewall buckling did not occur, a sharp increase in tire life of the conventional construction tires occurred. The difference in the sidewall deformations between the two types of tires could explain the difference in tire life. The main gear tires (17.00-20 and 20.00-20) did not show a dependency of tire life on deflection within the range of the total test cycles. It was noted that these larger size tires did not buckle in the sidewall at high deflections.

## SECTION IV

## CONCLUSIONS AND RECOMMENDATIONS

On the basis of the rolling resistance curves, the following general conclusions can be drawn. The rolling resistance of a tire is a function of velocity and deflection. For a given deflection, rolling resistance is nonlinear and increasing with increasing velocity. Although we can say that rolling resistance increases with increasing deflection, the scatter of the data makes it impossible to say whether the relationship is linear or nonlinear. Some parameter variations on the 9.50-16 tires indicate that increasing inflation pressure while maintaining a constant deflection results in decreasing rolling resistance (Reference Figures 5 and 6). Figure 7 indicates that as carcass temperature increases, rolling resistance decreases. Assuming that Figure 7 is representative, we can conclude that within the temperature range of the tire carcass under normal operating conditions, the effects of temperature on rolling resistance are not significant. (Peak carcass temperature for Type III tires under normal conditions vary from 100°F to 120°F). It must be emphasized that the rolling resistance curves generated in this program are results of data taken from one tire of each size and type, and as such, are only qualitatively valid.

Analysis of the results of the mission cycle testing (Reference Table II) indicates that at an approximate deflection of 40%, tire life for the conventional construction nose gear tires (9.50-16 and 12.50-16) changes sharply. (It was noted that at deflections greater than 40%, sidewall buckling occurred). It is concluded that operation at 40% deflection or greater is extremely hazardous since internal damage or construction defects could lead to catastrophic carcass failure without previous warning. The expandable tires of these sizes provided a noticeably increased life over the conventional construction tires at high deflections.

The main gear tires (17.00-20, 20.00-20) showed no difference in life between the two carcass construction types within the range of the test cycles of this program. On the basis of dynamometer testing, a 45% deflection on a freely rolling tire of these sizes is not harmful. It is expected that the tires would be removed because of tread wear well before 150 takeoffs and landings

are accomplished (These sizes completed 150 mission cycles on the dynamometer without failure). However, the effects of brake loads on the tire at high deflections are not quantitatively known. In general, brake loads on the main gear tires will reduce effective carcass life. These effects should be determined before implementing low tire pressures as a general procedure to provide increased flotation.

Therefore, it is recommended that reducing tire pressures to improve flotation not be adopted for conventional construction tires until 1) an on-board inflation-deflation system is developed to keep operation at high deflections to a minimum, and 2) a nondestructive test procedure is developed to inspect tires for internal defects or damage. The test results indicate that the expandable or folding sidewall carcass construction is more suited for operation at high deflections, and it is felt that a 45% deflection can be tolerated. However, since any defects or imperfections are greatly magnified at high deflections, an extremely tight and careful quality control would have to be exercised in tire production.

# APPENDIX

## MISSION CYCLE TEST CURVES

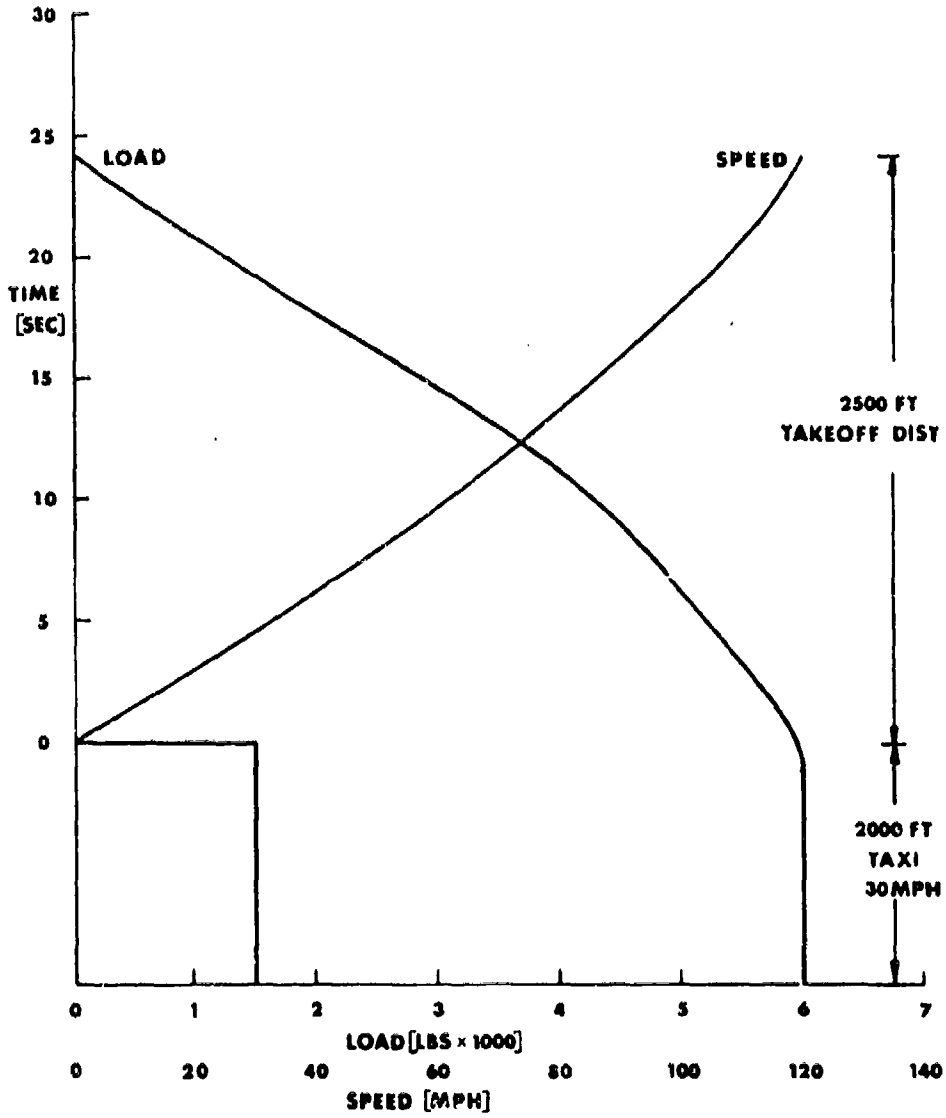


Figure 15. Mission Takeoff: C-123 NLG Tire (9.50-16)

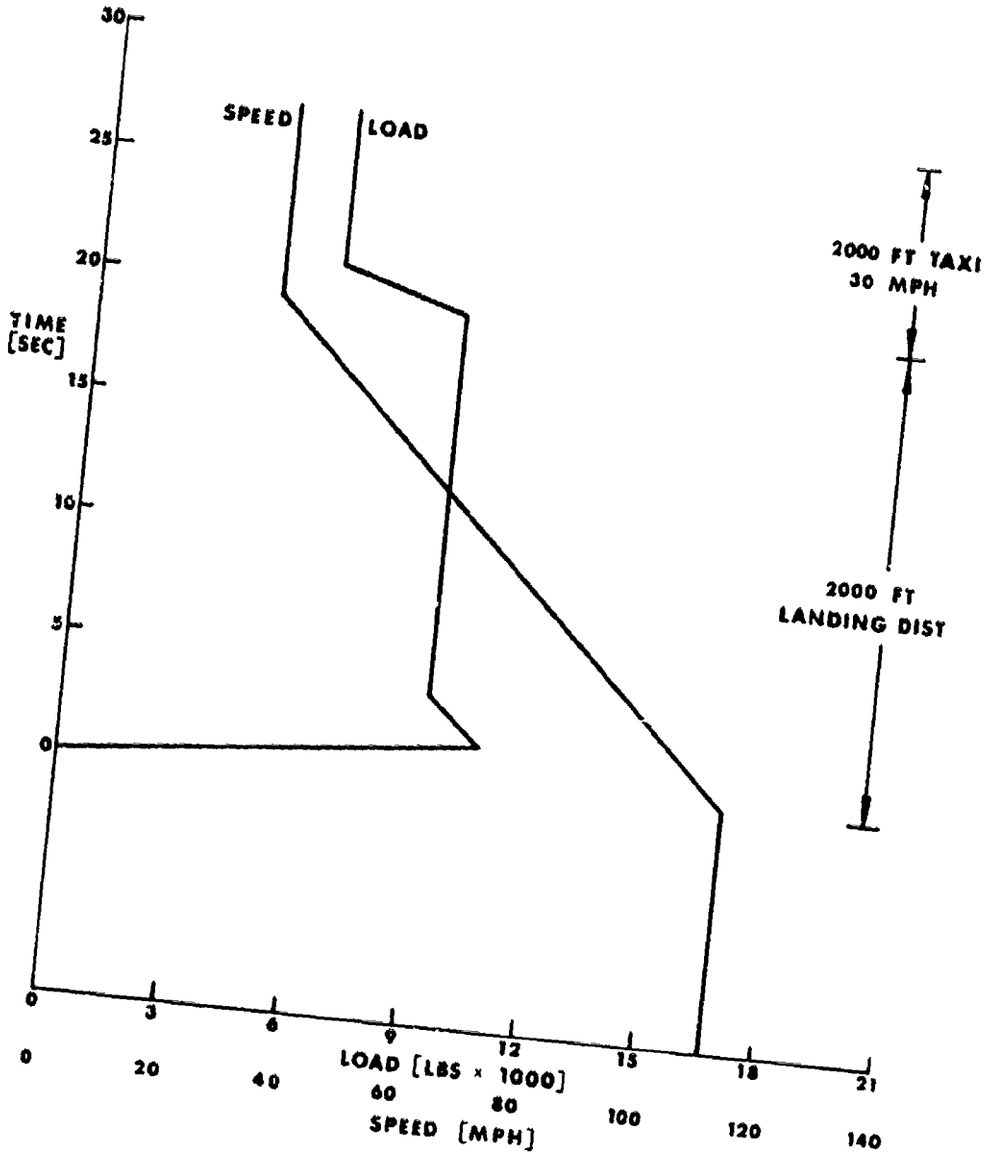


Figure 16. Mission Landing: C-123 NLG Tire (9.50-16)

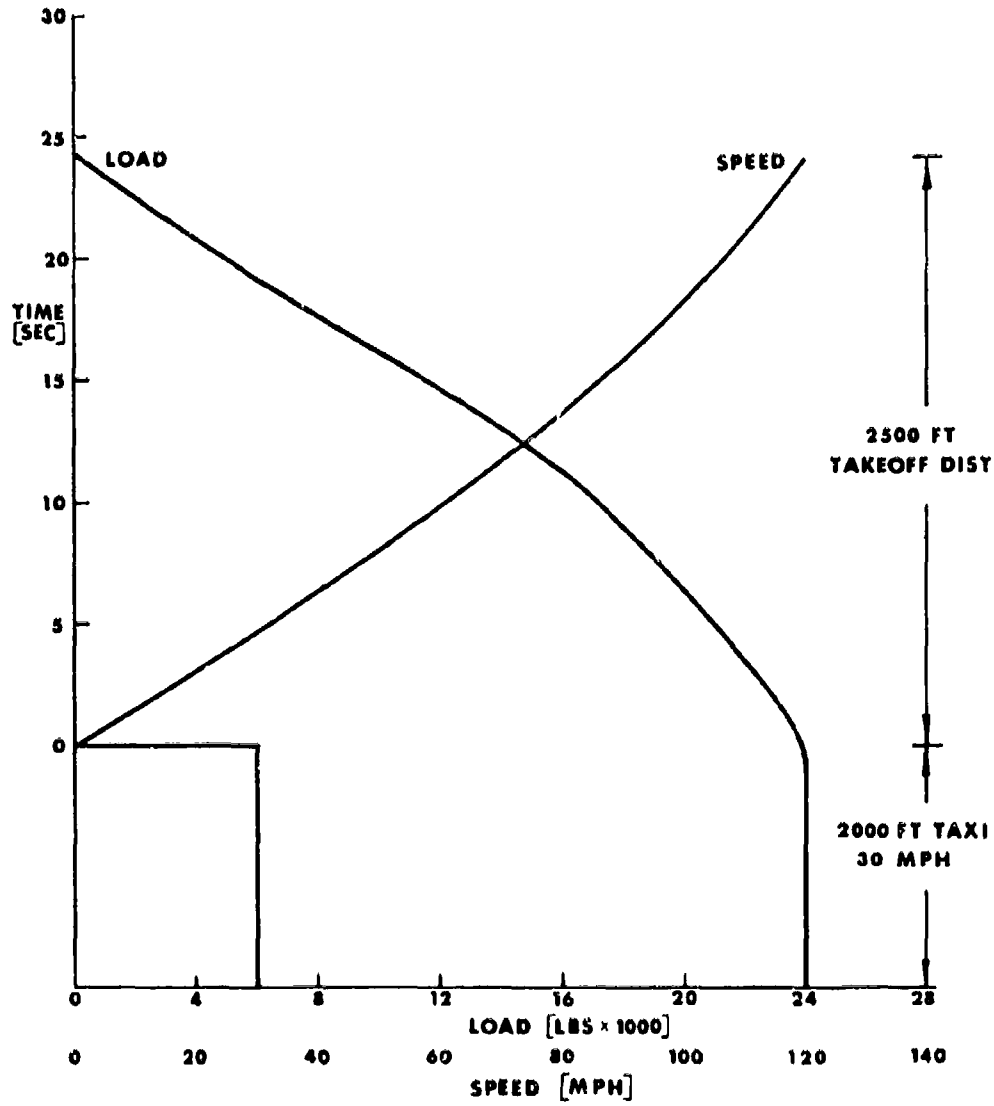


Figure 17. Mission Takeoff: C-123 MLG Tire (17.00-20)

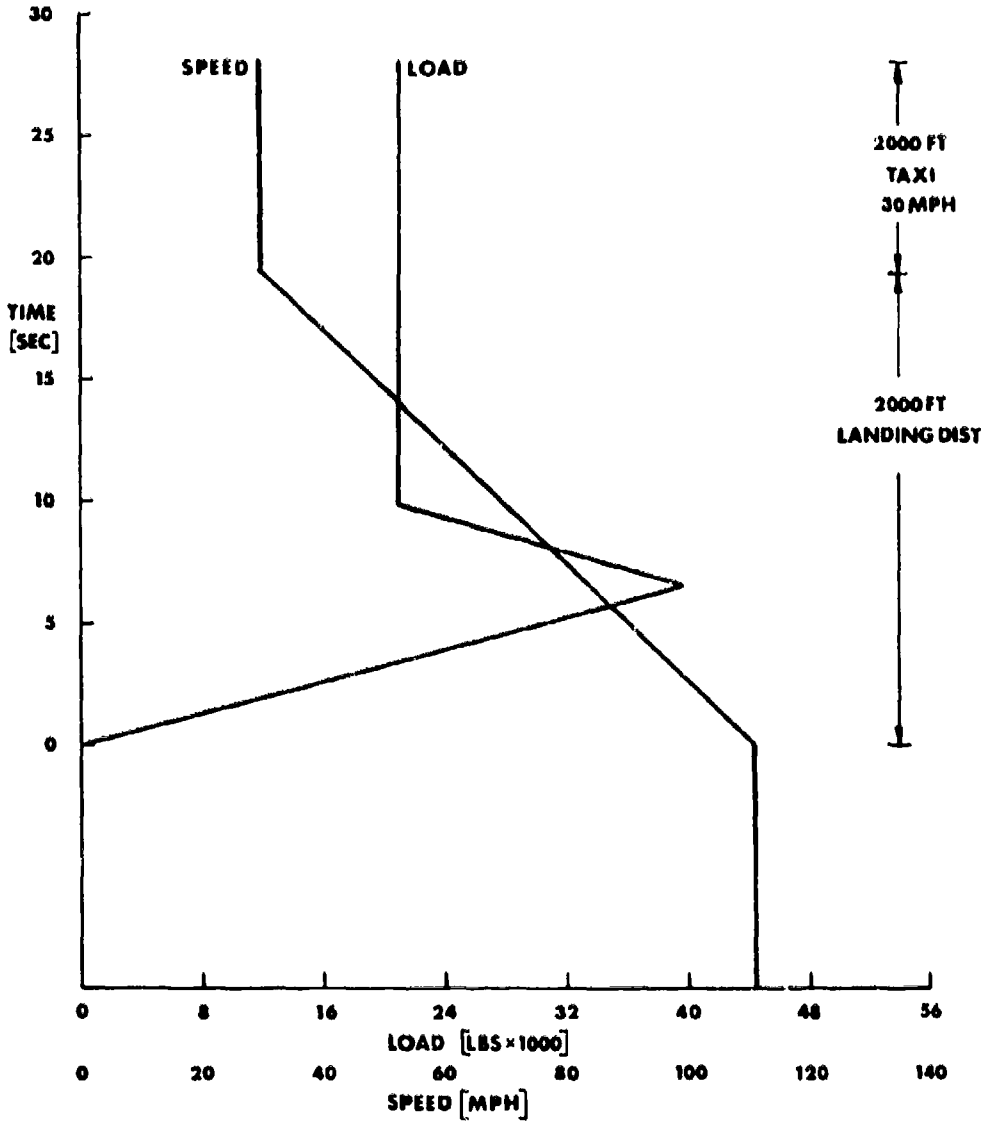


Figure 18. Mission Landing: C-123 MLG Tire (17.00-20)

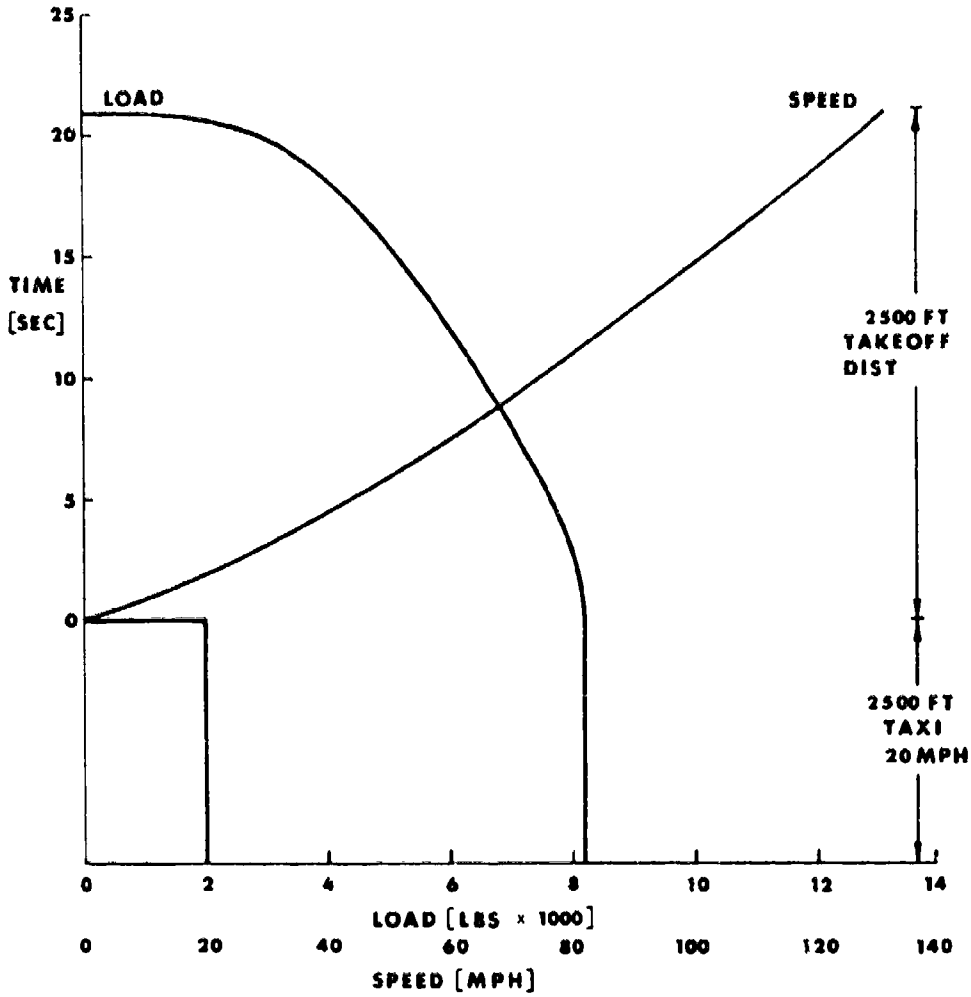


Figure 19. Mission Takeoff: C-130 NLG Tire (12.50-16)

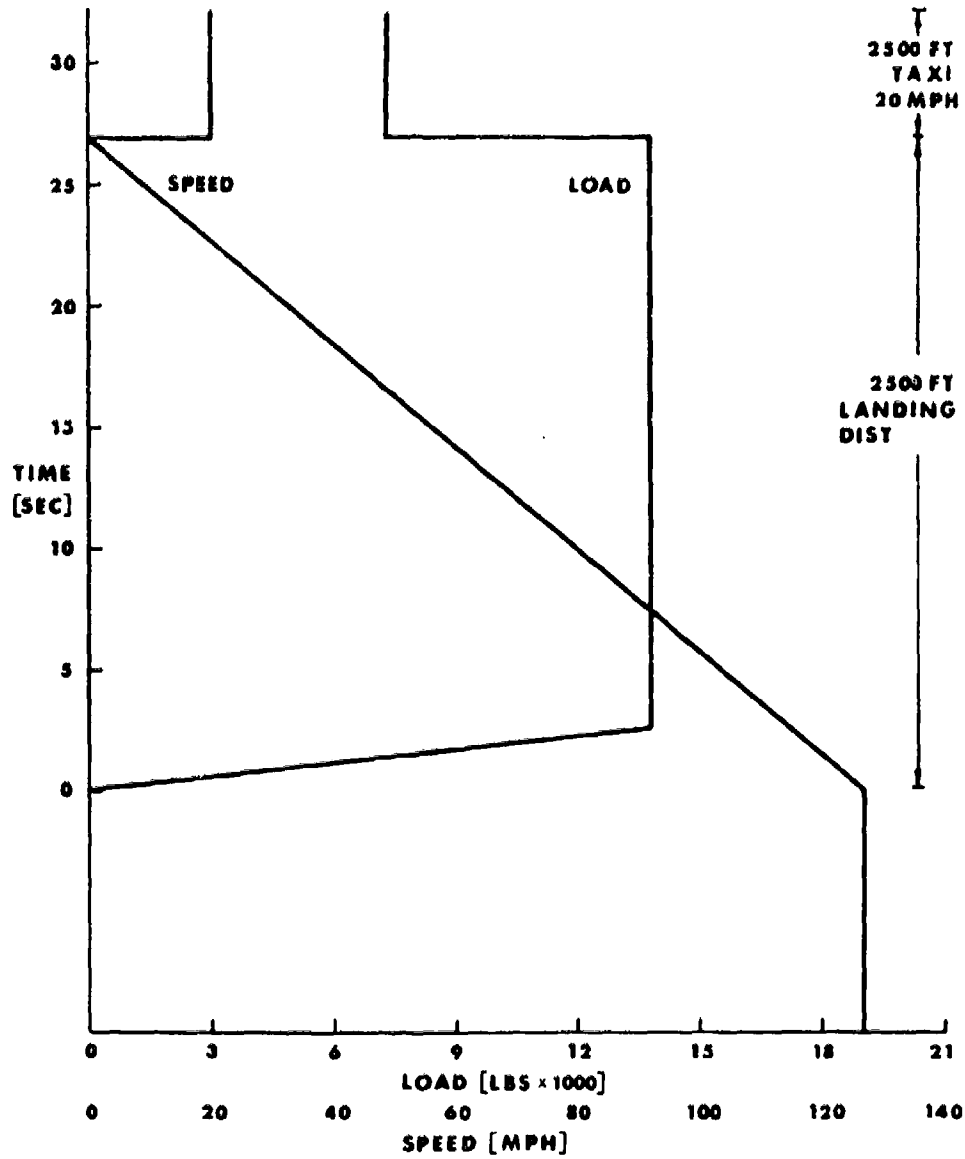


Figure 20. Mission Landing: C-130 NLG Tire (12.50-16)

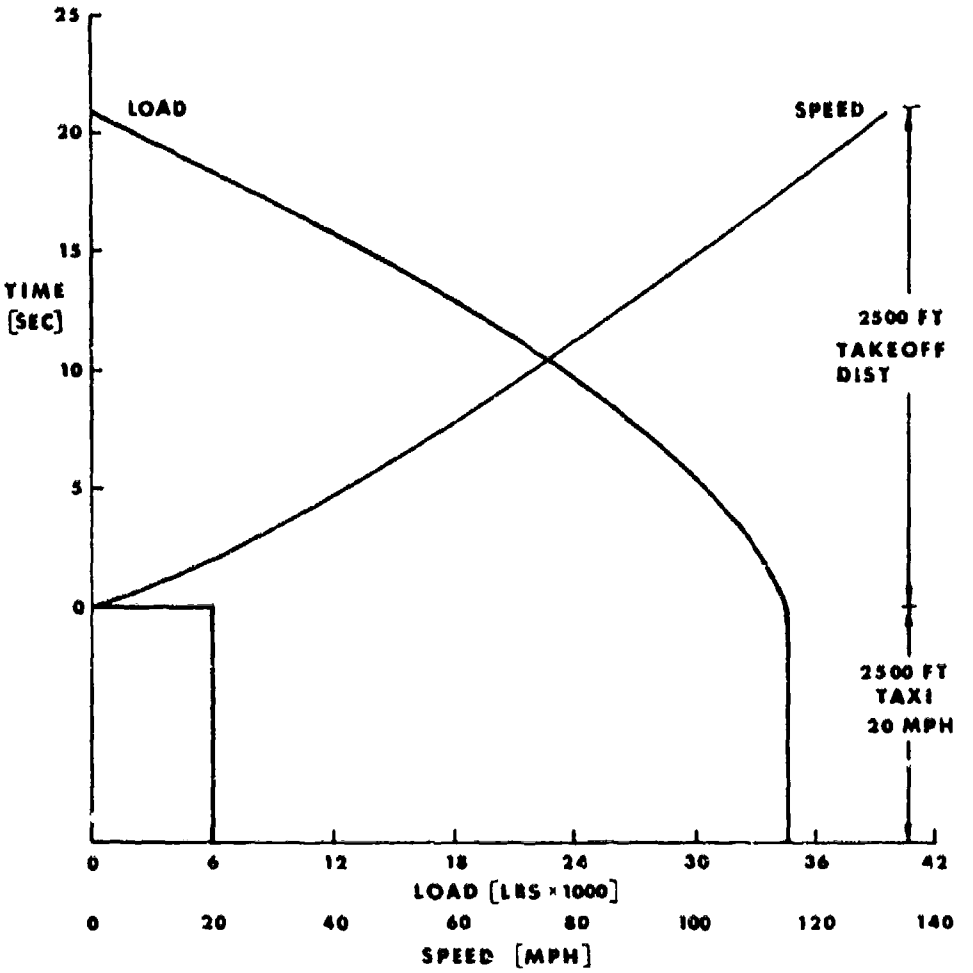


Figure 21. Mission Takeoff: C-130 MLG Tire (20.00-20)

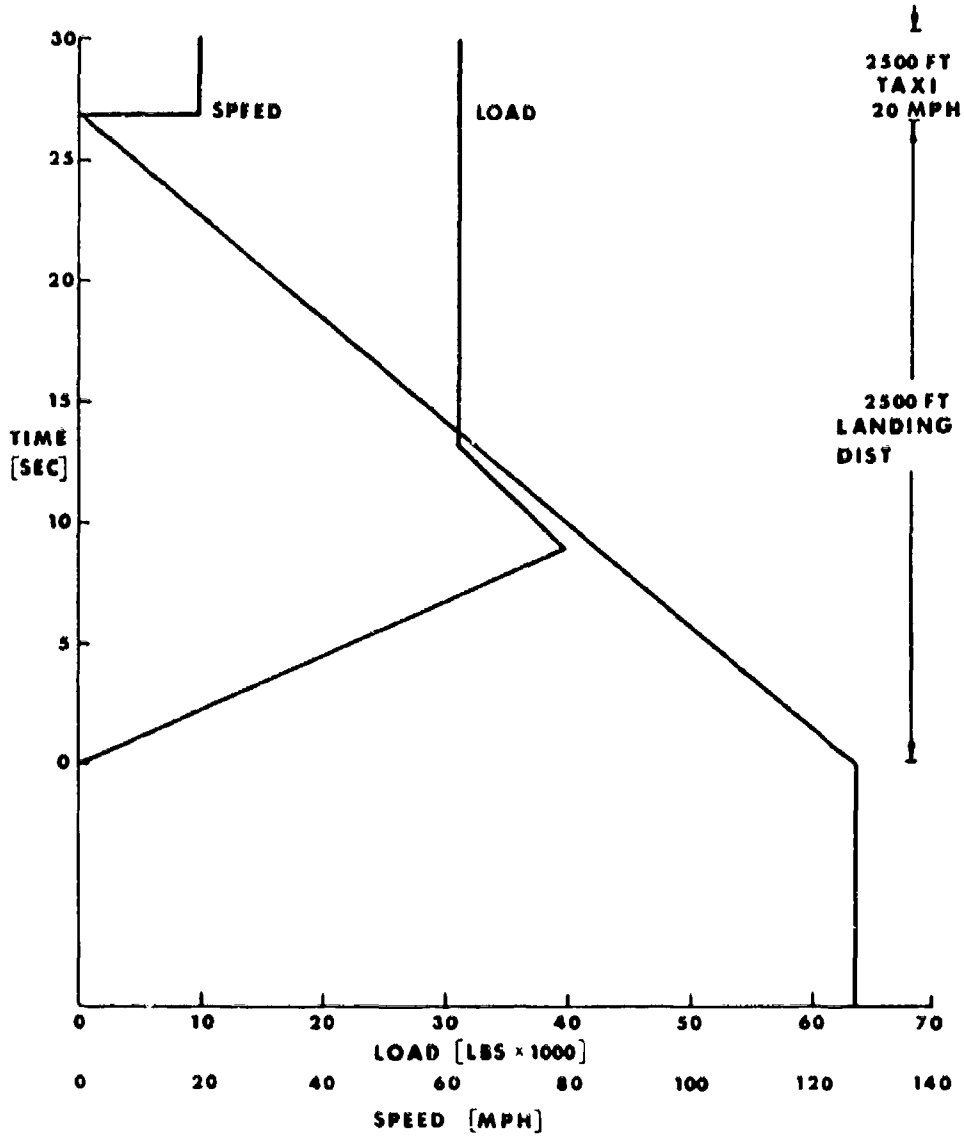


Figure 22. Mission Landing: C-130 MLG Tire (20.00-20)